Self-Assembly

International Edition: DOI: 10.1002/anie.201910603
German Edition: DOI: 10.1002/ange.201910603

Ion-Specific Assembly of Strong, Tough, and Stiff Biofibers

Nitesh Mittal[+], Tobias Benselfelt[+],* Farhan Ansari, Korneliya Gordeyeva, Stephan V. Roth, Lars Wågberg, and L. Daniel Söderberg**

Abstract: *Designing engineering materials with high stiffness and high toughness is challenging as stiff materials tend to be brittle. Many biological materials realize this objective through multiscale (i.e., atomic- to macroscale) mechanisms that are extremely difficult to replicate in synthetic materials. Inspired from the architecture of such biological structures, we here present flow-assisted organization and assembly of renewable native cellulose nanofibrils (CNFs), which yields highly anisotropic biofibers characterized by a unique combination of high strength (1010 MPa), high toughness (62 MJ m^{-3}) and high stiffness (57 GPa). We observed that properties of the fibers are primarily governed by specific ion characteristics such as hydration enthalpy and polarizability. A fundamental facet of this study is thus to elucidate the role of specific anion binding following the Hofmeister series on the mechanical properties of wet fibrillar networks, and link this to the differences in properties of dry nanostructured fibers. This knowledge is useful for rational design of nanomaterials and is critical for validation of specific ion effect theories. The bioinspired assembly demonstrated here is relevant example for designing high-performance materials with absolute structural control.*

Introduction

Nanoscale building blocks of biological origin exhibit outstanding mechanical properties due to strong interactions and directional assembly of the polymeric constituents.[1] Natural provenance and low density destined them to be the best material choice for designing future lightweight renewable materials for a range of advanced applications. Controlled arrangement of these building blocks into hierarchical materials with an attractive combination of stiffness, strength and toughness is of tremendous interest for researchers in materials science and engineering.[2] Fibers, in particular are desirable for a wide range of applications, such as lightweight construction in aerospace and automobiles, fuel cell electrodes and many others.[3] Additionally, fibers have high economic importance as the production of synthetic fiber accounts for more than 20% of overall plastic production which is valued at around $55 trillion in 2017.[4]

Multiple techniques such as wet or dry spinning have been developed to manufacture fibers from nanoparticles, however most of them just do not provide absolute control over the final nano- to macro structure.[1b,5] Bottom-up assembly using microfluidics is a promising strategy for designing structures with defined morphology.[1b,6] Self-assembly of colloids and nano-colloids is typically induced by screening or neutralizing the surface charges through the introduction of electrolytes or acids, where the destabilization of colloidal solutions is achieved from a long-known method of salting out or charge neutralization explained by the classical DLVO (Derjaguin–Landau–Vervey–Overbeek) theory.[7]

In the 1888, Franz Hofmeister described the capacity of different ionic species referred as kosmotropes or chaotropes to "create" or "break" the ordered structure of water based on the order of the anion and cation series, the so-called "Hofmeister series", following their ability to salt out proteins.[8] Since then, Hofmeister effects have shown general implications on phenomenon associated with bulk solutions

[*] Dr. N. Mittal,[+] Dr. K. Gordeyeva, Prof. L. D. Söderberg
Linné FLOW Centre, Department of Mechanics
KTH Royal Institute of Technology
Stockholm SE-100 44 (Sweden)
E-mail: dansod@kth.se
Dr. N. Mittal,[+] Dr. T. Benselfelt,[+] Prof. L. Wågberg, Prof. L. D. Söderberg
Wallenberg Wood Science Center
KTH Royal Institute of Technology
Stockholm SE-100 44 (Sweden)
E-mail: bense@kth.se
Dr. N. Mittal[+]
Department of Chemical Engineering
Massachusetts Institute of Technology
Cambridge, MA 02142 (USA)
E-mail: niteshm@mit.edu
Dr. T. Benselfelt,[+] Prof. S. V. Roth, Prof. L. Wågberg
Department of Fibre and Polymer Technology
KTH Royal Institute of Technology
Stockholm SE-100 44 (Sweden)
Dr. F. Ansari
Department of Materials Science and Engineering
Stanford University
Stanford, CA 94305-2205 (USA)
Prof. S. V. Roth
Deutsches Elektronen-Synchrotron (DESY)
22607 Hamburg (Germany)
[+] These authors contributed equally to this work.
Supporting information and the ORCID identification number(s) for the author(s) of this article can be found under: https://doi.org/10.1002/anie.201910603.

and at interfaces, which is important in the self-assembly of proteins, polymers, and inorganic or organic nanoparticles.[9] The large diversity of different ions provide numerous opportunities to rationally design engineering materials, such as regulating the gelation process of supramolecular hydrogels.

Herein, we apply the accumulated knowledge of Hofmeister effects, today known as specific ion effects, to the state-of-the-art microfluidics-based assembly process, where CNF dispersions are subjected to flow fields to orient the fibrils along the flow direction, followed by gelation to fabricate nanostructured materials with superior mechanical properties. This nanostructure is inspired by the aligned fibrillar structure in the S2 layer of wood fiber walls.

Experimentally, we show that the ion-induced assembly of cellulose nanomaterials can moderately reproduce the trends in the mechanical properties as indicated for different ions in the Hofmeister series. First, our analysis of tensile properties shows that choice of ions results in variations in the strength, toughness and stiffness of dry nanostructured CNF biofibers. Furthermore, the dynamic structural features of hydrogels tested by rheology indicate variations in the storage modulus that could be linked to the making and breaking of the nanostructure under shear forces due to the effects of the specific ions. The properties of the hydrogel influence the nanostructure development during wet to dry transition, and these observations clarify the variations in properties of dry CNF fibers. In accordance with recent work from our group that studied the assembly of CNFs based on diffusion of protons,[6b,10] we here suggest that anions such as Cl^-, Br^-, ClO_4^-, HSO_4^-, $H_2PO_4^-$ are included in or expelled from the supramolecular hydrogels to minimize the perturbation of water. Thus, these anions participate in the self-assembly through direct or indirect influence on CNF interactions. Variations in the mechanical properties are related to the structural discrepancies induced by different ions, based on the most reliable explanations for the Hofmeister series and specific ion effects.

Results and Discussion

Macroscale bio-based fibers (biofibers) are prepared from flow-induced alignment of nanofibrils followed by the assembly through surface-charge controlled sol to gel transition.[6b] In this hydrodynamics-based approach, dispersed nanofibrils (Supporting Information, Figures S1 and S2) are aligned in the flow direction with the help of flow fields before inducing a self-assembly to lock the nanostructure into a metastable colloidal glass.[6b,11] The goal is accomplished by using an elongational flow fields-based double flow-focusing geometry (Figures 1 a and S3) where the channel geometry consists of a core flow fluid and two sheath flow fluids[6b,12] In the core flow, a dispersion of surface charged CNFs is injected where the nanofibrils are free to translate due to electrostatic repulsions and Brownian rotary diffusion.[13] The first sheath flow consists of deionized (DI) water which aligns the fibrils in the flow direction[6b] and also protects fibrils from shear close to the channel walls. The alignment of fibrils is quickly

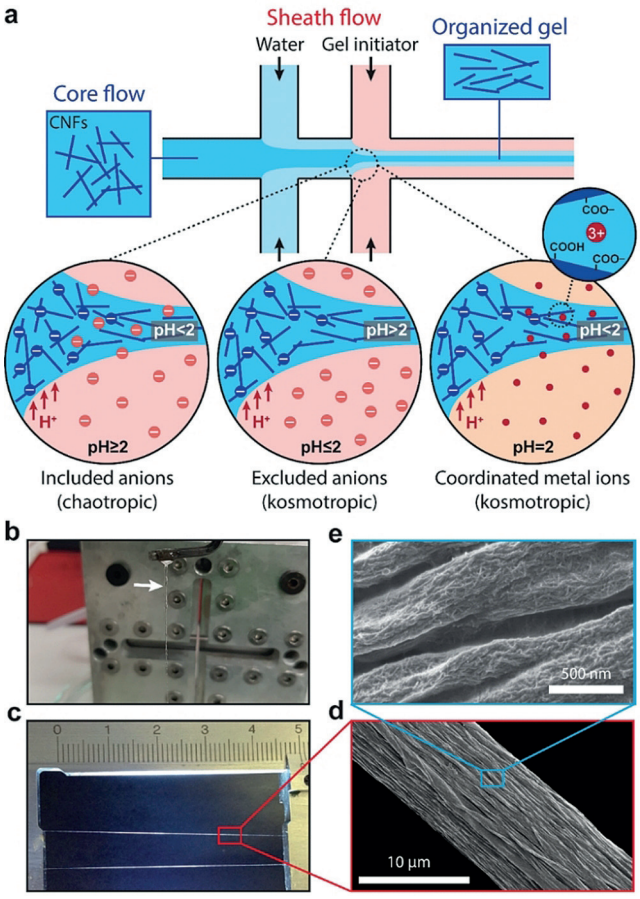

Figure 1. Biofiber assembly. a) Schematic of the channel setup used to achieve flow-induced alignment and illustration of three alternative locking mechanism. b) Picture of the gel thread after the assembly. c) Picture of the dried CNF biofiber. d) and e) Electron micrographs of the fibers.

diminished due to the Brownian motion; hence it is important to lock the nanofibrils in the aligned state before the system approaches isotropy. The second sheath flow thus consists of a gel initiator that reduces the double layer repulsion between the nanofibrils mainly through a protonation of the carboxyl groups but also through an increased ionic strength. This induces the self-assembly of the fibrils into a well-packed colloidal glass with maximized CNF-CNF contacts (Figure 1 b). Van der Waals forces and arrested translational and rotational movement are the presumed mechanism behind the gel formation. The obtained continuous gel threads are subsequently picked up from the DI water bath, held at their ends and air-dried (Figure 1 c). Characterization of the CNFs fiber surface with scanning electron microscopy (SEM) (Figures 1 d and e) sampled in the longitudinal direction showed highly anisotropic and densely packed organization of fibrils.

Using this assembly technique, we explore three alternative gel initiation mechanisms (Figure 1 a), including acids that are either chaotropic or kosmotropic, or a Lewis acid in the form of $FeCl_3$ with the highest propensity to coordinate ligands on the surface of the CNFs to form complexes which crosslink fibrils in strong hydrogel networks.[9d,14] Chaotropic

ions disrupt the order of water, have a low hydration enthalpy, are relatively larger, and generally more polarizable, whereas kosmotropic ions increase the order of water, have a high hydration enthalpy, are relatively small, and generally less polarizable. In the specific ion effect theories, the hydration enthalpy and the polarizability of ions have been suggested to explain the Hofmeister series by direct interactions with water and dispersed colloids.[15]

To understand how CNF hydrogels are affected by the gel initiation mechanisms, we must elucidate the properties of CNF surfaces. Cellulose should be considered chaotropic since kosmotropic polymers are typically soluble in water. Furthermore, most carbohydrate polymers have a positive chi-parameter which means that their interaction with water is typically not stronger than interactions between water molecules.[16] However, the added carboxyl groups on the surface of CNFs are strongly hydrated, but at a charge density of 0.6 mmol g^{-1}, the coverage is moderate and at low pH, most of the carboxyl groups are protonated and the chaotropic properties dominate.[17]

Chaotropic ions accumulate near chaotropic surfaces, such as CNFs, in order to minimize the perturbation of water (Figure 2a) or are adsorbed via ion-surface dispersion interactions (Figure 2b), whereas kosmotropic ions accumulate in the bulk water solution (Figure 2a) or at kosmotropic surfaces for the same reason.[9d]

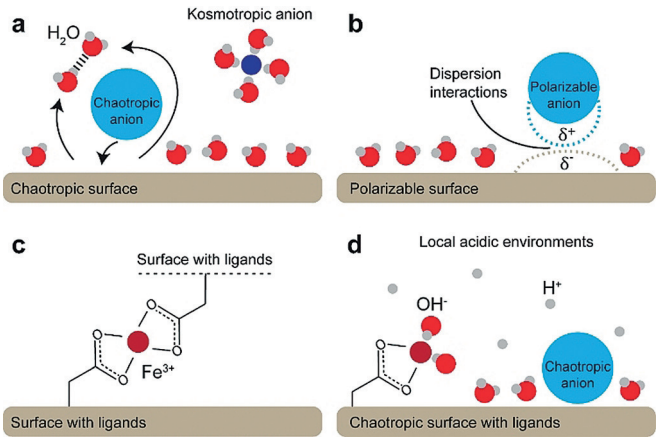

Figure 2. Specific ion effect schematics. a) Chaotropic or kosmotropic ions are accumulated at or excluded from surfaces. b) Polarizable ions adsorb to surfaces via dispersion interactions. c) Coordination complex formation. d) Local acidic environments induced by coordinated or adsorbed ions via balancing of ionic species similar to the Donnan equilibrium.

Fe^{3+} ions are highly hydrated and coordinate water, but the entropy of the system can be increased by exchanging the tightly bound water with something which has fewer degrees of freedom, such as carboxyl ligands on the CNF surface. Metal ions therefore accumulate inside the hydrogels by a combination of electrostatic attraction and dative covalent coordination bonds regardless of their kosmotropic nature.[9d,14b] For this to conform to the specific ion effect theories which attempt to explain the Hofmeister series by the perturbation of water, we can no longer use average properties of the CNFs but must realize that specific groups, for example, carboxyl ligands, enable specific ion binding.

Furthermore, chaotropic and kosmotropic anions (Figure 2d), or coordinated Fe^{3+} (Figure 2c) induce a local environment (Figure 2d).[18] The cause of the local environment is similar to the Donnan equilibrium for fibers in pulp, with the fiber surface or the hydrogel surface acting as a semipermeable membrane through which ions migrate depending on their specific properties (Figure S4).[18] Accumulation of chaotropic ions close to chaotropic CNF surfaces inside the hydrogel thus increase the local concentration of acid, whereas excluded kosmotropic ions result in a lower concentration of acid inside the hydrogel than in the bulk solution (Figure 1a). An inevitable consequence of this Hofmeister effect is that the pH measurement using glass electrodes is ion-specific since chaotropic acids accumulate at the surface of glass electrodes and induce a local pH.[19] There are therefore slight uncertainties in pH measurements, which are indeed difficult to avoid and moreover diminish small specific ion effect variations since the pH is not exactly what we measure.

The above information allows us to predict how different gel initiators affect the properties of the hydrogels (illustrated in Figure 1a). The biofiber properties can subsequently be related to the properties of the hydrogel in order to rationalize ion-specific assemblies of CNFs using flow-induced alignment.

For a comprehensive understanding of how specific ions affect the assembly process and hence the mechanical properties of the fibers, we first prepared fibers using three different acids: HCl, H_2SO_4, and H_3PO_4 at pH 2 and a CNF concentration of 0.3 wt % (Figure 3a). A linear elastic region followed by a plastic region is observed in all stress-strain curves (Figures 3a and b). The yield point in the stress-strain curves highlights the transition from elastic to plastic deformation and is most probably associated with the relative sliding of nanofibrils.[6b,20] Some fibers have a secondary yield point at high strain which has been hypothesized to be governed by cooperative entanglements and release of nanofibrils from such structures.[21]

CNF fibers prepared using HCl results in stiffer fibers compared to those prepared using H_2SO_4 and H_3PO_4, with a modulus and ultimate strength of $\approx$57 GPa and $\approx$1010 MPa, respectively (Figure 3a). The obtained modulus and ultimate strength with H_3PO_4 is $\approx$38 GPa and $\approx$740 MPa (Figures 3b and e). Surprisingly, despite significant variations in the elastic modulus of the fibers, the orientation of nanofibrils remain almost the same as determined by wide-angle X-ray scattering (WAXS) (Figure S5). The orientation index[22] measured for HCl, H_2SO_4 and H_3PO_4 is 0.850 ± 0.003, 0.867 ± 0.007 and 0.847 ± 0.012, respectively. The large variation in terms of mechanical properties highlights that the process of flow-induced assembly results in a certain level of orientation of the nanofibrils,[6b] whereas the properties of the fibers are governed largely by the specific properties of the anions of acids that are used as gel initiators.

Infrared spectroscopy shows that a large portion of the carboxyl groups of CNFs are still in a dissociated state

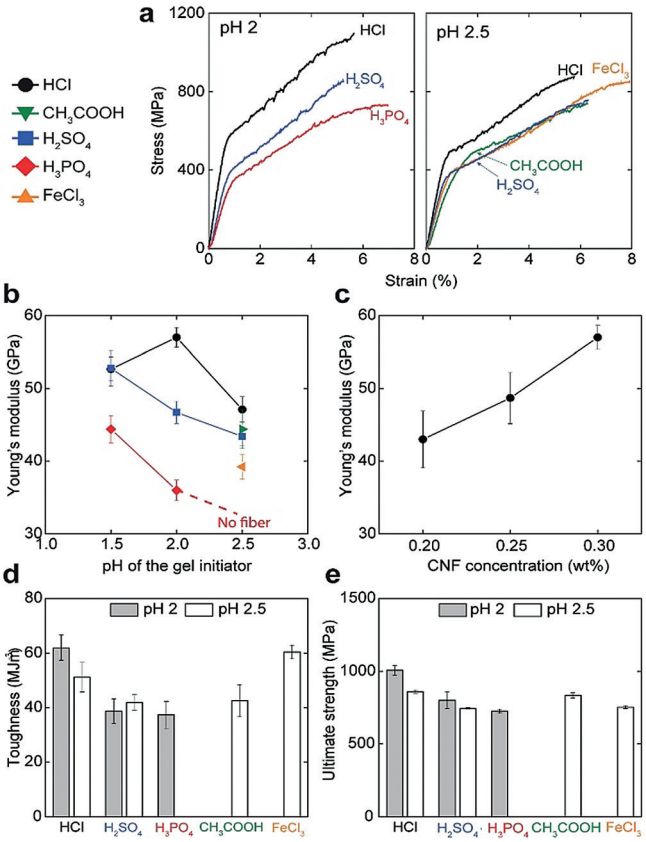

Figure 3. Tensile mechanical properties of CNF biofibers. a) Representative stress-strain curves of fibers prepared at pH 2 and 2.5 of the gel initiator and 0.3 wt% CNF concentration. Young's modulus as a function of b) pH of the gel initiator and, c) CNF concentration for HCl. d) Toughness and e) ultimate strength of fibers prepared with different gel initiators at pH 2 and 2.5. The different acids are referred to by the color and shape of the data points. Error bars are 90% confidence intervals based on at least 10 different measurements for each type of sample. All the measurements are done at 50% RH.

($1600\ cm^{-1}$) in fibers prepared at pH 2 (Figure S6a), which shows the importance of considering local environments.

For a thorough understanding on the ion-specific properties of our materials, we proceeded to prepare fibers with four different gel initiators at pH 2.5 and a CNF concentration of 0.3 wt% (Figure 3a). Fibers prepared using HCl resulted in the stiffest fibers similar to the case at pH 2. Among the acids HCl, H_2SO_4, and CH_3COOH, the lowest stiffness was obtained with CH_3COOH. Surprisingly, we did not manage to obtain fibers with H_3PO_4 at pH 2.5 since the gel threads were too weak to sustain air–water interfacial tension while lifted out of the water bath. The compiled data in Figure 3b shows that a lower pH lead to stiffer and stronger fibers, with the exception of HCl at pH 1.5

Apart from anionic acids, fibers were also prepared using $FeCl_3$ of pH 2.5 and an inferior modulus (39 ± 2) but enhanced ultimate strength (834 ± 21) and strain-to-failure ($\approx 8\%$) was obtained (Figure 3a). This is related to the dative covalent coordination complexes which affect the relaxation and consolidation of the aligned CNF structure and hence the morphology of the fiber upon drying.[23] Interestingly, unlike Fe^{3+} treated isotropic films, the carbonyl vibration of Fe^{3+} treated oriented fibers show complete dissociation of the carboxyl groups (Figure S6b).[9d] Fibrils in parallel configuration favors complexation which pushes the equilibrium towards dissociation regardless of the local acidic environment.

To extend the property range of these fibers, we tuned the concentration of CNFs in the dispersions and observed that the stiffness increased proportionally to the solids content of the hydrogel, from a stiffness of ≈ 57 GPa and a strength of 1010 MPa at 0.3 wt% to a stiffness of 43 GPa and a strength of 770 at 0.2 wt% (Figure 3c). The decrease in stiffness and ultimate strength is related to the decreased solids content of the gel thread that may lead to heterogeneously packed networks of the nanofibrils in the dried fiber. However, it was experimentally challenging to obtain reliable statistics on the density measurements of our materials. Nevertheless, these results show that the stiffest materials also tend to be the strongest by ensuring adequate load transfer and cohesion between the nanoscale constituents.[1a]

Apart from the strength and stiffness, we also evaluated the work of fracture (toughness) defined as the area under stress-strain curves (Figure 3d). The CNF fibers prepared with HCl at pH 2 has an exceptionally high toughness of $62 \pm 6\ MJ\ m^{-3}$. Such high toughness has not yet been reported for any cellulosic material prepared with other known fabrication techniques (Table 1). In a wider perspective, the mechanical properties of our fibers are superior to all commercially available cellulose fibers (Viscose, Cordenka, Lyocell, and Ioncell-F fibers) and all other nanocellulose fibers prepared with dry or wet spinning techniques (Table S1).[6b,24] Notably, our CNF fibers also outperform the mechanical performance of dragline spider silk, which is often consider as a gold standard for biopolymeric materials, which has a similar strength and toughness but up to 10 times lower stiffness.[25]

Table 1: Comparison of the toughness of our fibers with the cellulose fibers prepared with other techniques.

Cellulose Fiber/Material Type	Preparation Method	Toughness [$MJ\ m^{-3}$]	Reference
Viscose	Dissolution and regeneration	33	Adusumali, et. al[24c]
Modal	Dissolution and regeneration	37	Adusumali, et. al[24c]
Lyocell	Dissolution and regeneration	35	Adusumali, et. al[24c]
Rayon	Dissolution and regeneration	41	Adusumali, et. al[24c]
Flax	Liberation from the stem	16.7	Adusumali, et. al[24c]
Bacterial Cellulose	Wet twisting	45	Gao, et. al[26]
CNF	Wet extrusion (Syringe)	31	Mohammadi, et. al[27]
Bacterial Cellulose Sheets	Surface selective dissolution	13	Soykeabkaew, et. al[28]
CNF Ribbon	Hydrogel stretching	19	Tang, et. al[22]
TEMPO-oxidized CNF	Wet extrusion (Syringe)	8.7	Walther, et. al[29]
Carboxymethylated CNF	Microfluidics	62	Present Work

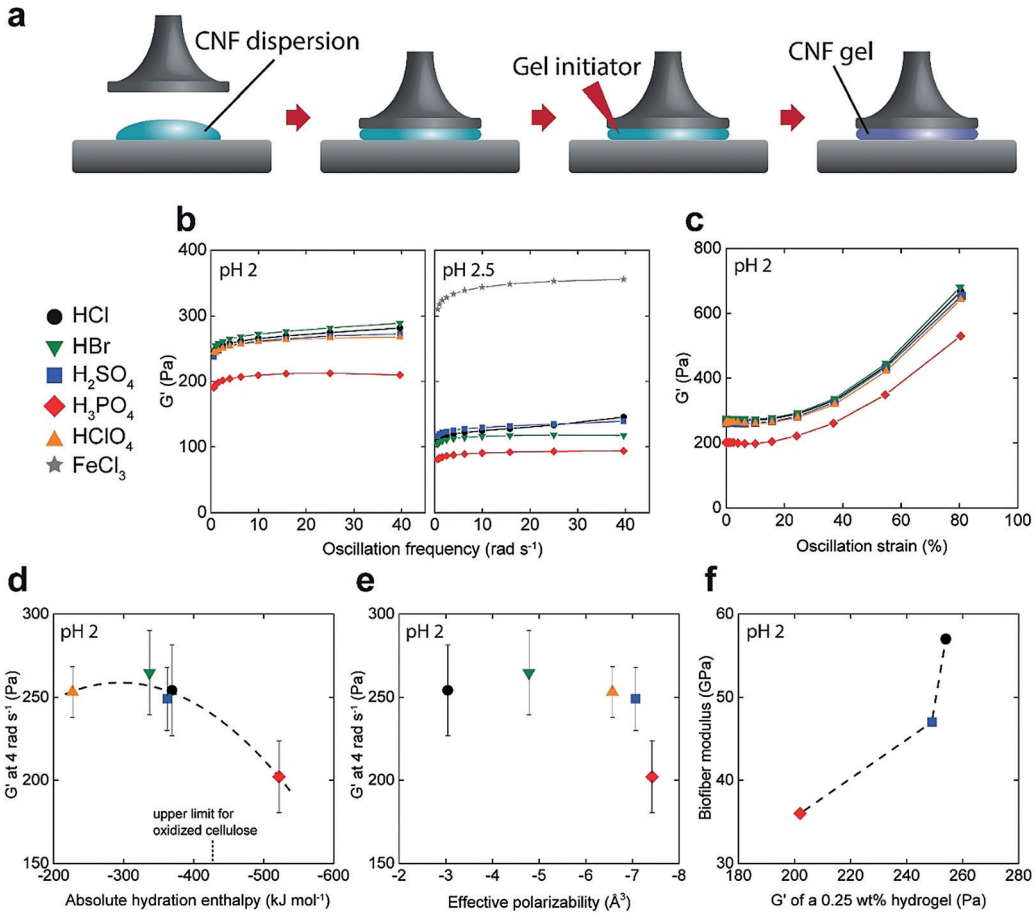

Figure 4. Rheological properties of CNF hydrogels. a) The sample preparation and instrumental setup. b) Frequency sweeps at pH 2 and 2.5. c) Amplitude sweep at pH 2. d) Relationship between storage modulus and absolute hydration enthalpy of the anion. e) Relationship between storage modulus and effective polarizability of the anion. f) Relationship between the biofiber modulus and the storage modulus of the hydrogel. The different acids are referred to by the color and shape of the data points. Error bars are 90% confidence intervals based on at least 4 different measurements for each type of sample.

We proceeded to study the rheological properties of hydrogels formed by the different gel initiators (procedure depicted in Figure 4a) in order to relate the stiffness and strength of the CNF fibers to the ion-specific properties of the hydrogels. The hydrogels have the typical oscillatory frequency response of self-supporting hydrogels (Figure 4b) and showed a strain stiffening behavior (Figure 4c). A lower pH of the gel initiation solution results in a greater storage modulus of the hydrogels (Figure 4b) and stronger fibers (Figure 3b), which in turn suggests that there is a strong relationship between the properties of the hydrogel and the dry fiber, even though the rheological investigations are made for an unoriented CNF gels and the fibers are indeed oriented. There might be several explanations to this correlation which merits further investigations.

H_3PO_4-initiated gels showed the lowest storage modulus which is related to an inferior stiffness of the dried fibers (Figure 2b). Thus, at high pH, we were unable to form hydrogels strong enough to be lifted from the water bath when using H_3PO_4. $FeCl_3$, on the other hand, greatly increases the stiffness of the hydrogel due to the coordination with carboxyl groups and other detailed molecular interactions described elsewhere,[9d,30] but interestingly this elevated storage modulus of $FeCl_3$ initiated gels was not translated into fiber stiffness. It appears that excessive strength of the gel networks is not beneficial in the wet to dry transition, and can for example prevent further alignment of fibrils or create a more porous structure of the dry fibers. A further example of this discrepancy is the reduced stiffness of the fibers prepared by HCl at pH 1.5 compared to those prepared at pH 2 (Figure 3b), although pH 1.5 gave stronger hydrogels. The fibers formed by $FeCl_3$ show the highest toughness (Figure 3d) and it can be suggested that this is due to a more porous network with hidden length scales, the hydration of Fe^{3+} (Figure S6b), or directly related the sacrificial energy of breaking coordination complexes since this toughness was not achieved with HCl at pH 1.5.

In order to characterize the specific ion effects, we have related the properties of the hydrogels to the inherent properties of the different ions. Starting with ion hydration as a measure of water perturbation, we use acids with a broad range of hydration enthalpies (Figure 4d).[31] $H_2PO_4^-$, the most hydrated and hence most kosmotropic anion, is according to the theory excluded from the hydrogel and the

following charge balance (opposite to Figure S1) leads to a higher pH inside the gel which is associated with less stiff hydrogels (Figure 4a) and fibers (Figure 3b). This is supported by elemental analysis which shows that the portions of Cl or S that migrates into fibers are similar, whereas a smaller portion of the available P enters the fibers (Table S2).

For the other ions, no significant relationship between storage modulus and hydration enthalpy is observed, and this can be related to the state of hydration of the CNFs. Acetate or formate, as models for carboxyl groups on the CNFs, have hydration enthalpies on the order of 420–430 kJ mol^{-1}, which is hence the upper limit for the hydration of the CNFs. Ions with hydration enthalpy below this thus accumulate inside the hydrogels and reduce the local pH which translates into stronger hydrogels. The same argument can be adapted based on the hydration entropy of the anions (Figure S7), which follow a similar trend as the hydration enthalpy. The hydration enthalpy and the pK_a of the acids are strongly related (Figure S8), with H_3PO_4 having the highest pK_a of 2 and $HClO_4$ the lowest of close to 10. The balance between associated and dissociated acids is also important in terms of water perturbation and ion migration, and in this respect H_3PO_4 solutions at pH 2 have the greatest portion of associated acids (Table S2).

Moisture sorption into dried hydrogel samples, which reduces the stiffness of CNF materials,[24b] also follows the hydration of the different ions (Figure S9 and Table S3). However, the subtle differences in water sorption cannot alone explain the differences in mechanical properties of the biofibers.

We continued to study the polarizability of the anion as a measure of ion-surface dispersion interactions. Although the introduced anions have variations in effective polarizability,[15c,32] we found no relationship with regards to the storage modulus of the hydrogels (Figure 4e). For example, $H_2PO_4^-$ and HSO_4^- have close to the same polarizability, but $H_2PO_4^-$ initiate significantly softer hydrogels which implies that the dispersion is not decisive in these systems. Ion-surface dispersion interactions are mediated by the difference in dielectric response of the surface and the medium.[15c] Surfaces with low permittivity, such as oil (2) or cellulose (3–7), in relation to water (80) result in strong adsorption of polarizable ions, and we therefore assume that most of these anions to certain degree adsorbs to CNFs. Instead the hydration-controlled accumulation and exclusion of ions dictates if adsorption is possible.

The general trend is that a stiffer hydrogel result in a stiffer fiber (Figure 4f). However, H_2SO_4 produces weaker fibers than expected based on gel stiffness, which indicates that there are other mechanisms involved. A property that differentiate H_2SO_4 from the other acids is the secondary pK_a just above 2, and hence a significant amount of SO_4^{2-} exists in the gel initiation solution (Figure S8). SO_4^{2-} is significantly more hydrated than HSO_4^- and the intricate balance between monovalent and divalent anions, such as their accumulation or exclusion, or the lower salt concentration should be considered as a cause of the inferior stiffness of these fibers.

To gain further insight of how accumulation of different ions in between CNFs affect the fibril-fibril contacts, we prepared isotropic hydrogel networks using vacuum filtration.[33] We added the ions to these networks in two ways: soaking dried network in the gel initiation solution (Figure 5a) or soaking the filter cake before drying (Figure 5b). These isotropic CNF networks were only marginally affected by the specific ions (Table S4). This shows that the structure in the oriented fibers is more sensitive to specific ions, which is reasonable since the fiber properties are determined by contact between fibrils surfaces, whereas random CNF gels are primarily determined by the properties of the network.[30] Thus accumulated or adsorbed ions which disrupt fibril contacts is detrimental for oriented fibers (Figure 5c) while random CNF networks retain a fixed interlocking regardless of gel initiator (Figure 5d). Consequently, the sizes, hydration and other properties of adsorbed or accumulated ions are important since, for instance, larger ions are reasonably more disruptive (Figure 5c) which has been shown for bulky counter-ions.[34] This can potentially also explain why H_2SO_4 lead to less stiff fibers compared to HCl despite the observation that these hydrogels have more or less the same storage modulus (Figure 4f and Figure 3b). The same reasoning is valid in the case of H_3PO_4 and $FeCl_3$ where considerable amounts of ions block fibril contacts (Table S2).

To evaluate the extractability of the ions as a measure how tightly they are bound inside the fibril network, we used ion chromatography. In this experiment, ions are extracted with water from the dry films in Figure 5b, and Table 2 shows that the extractability in moles per weight of Br^-, Cl^-, and $H_2PO_4^-$

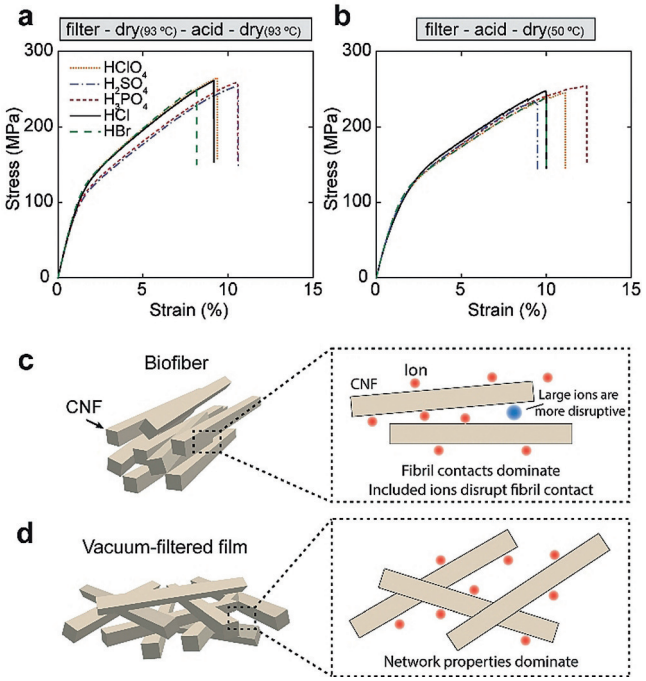

Figure 5. Mechanical properties of isotropic CNF films. a) and b) Representative stress-strain curves for films with different treatments referred to by color and structure of the line. c) and d) Illustrations of the organization in a biofiber (c) and a vacuum filtered film (d) and how specific ions presumably affect these materials. Data is averaged for at least 4 samples of each type. All the measurements are performed at 50% RH.

Table 2: Extractability of ions measured by ion chromatography.

Ion type	% wt/wt	% mol/wt
Bromide	0.29	0.0036
Chloride	0.16	0.0045
Sulfates	0.15	0.0015
Phosphates	0.58	0.0060

follow the Hofmeister series and the thermodynamics of hydration, that is, Cl^- is easier to extract than Br^-. The amount of HSO_4^- is lower than the other due to the divalent nature of sulfuric acid (Table S2).

Conclusion

In conclusion, our CNF biofibers stand out from other known biofibers based on their superior mechanical performance. Our results show that the process of flow-induced alignment and assembly lead to a certain level of orientation of the nanofibrils and that the divergence in mechanical properties of the biofibers is governed largely by a combination of pH of the gel initiator, CNF concentration, and specific ion effects. The direct influence of different ions is evident from WAXS results, which shows no difference in the orientation of crystal planes of biofibers prepared using different gel initiators. It is thus important to consider the accumulation of ions in proximity to the nanofibrils and the resulting local pH as well as disrupted fibril contact. The common description of how the presence of anions or cations perturb water molecules and how this dictate the accumulation of ions in the wet nanoparticle networks, invoke some notion of nanostructure making or breaking,[35] although a thorough understanding of this remains elusive. Here, we have tried to provide an understanding of these ideas by describing the variations in the mechanical properties of both hydrogels and CNF fibers with the choice of ions that potentially is coupled to the differences in the nanoscale networks. Though with the limitations of the experimental tools, it is challenging to determine the exact state of ions inside the network structure. Another picture that emerges from the present results is that ions potentially do not disrupt isotropic networks with larger pore sizes, rather the effect is more observable in oriented structures where the cohesion is mainly governed by fibril contacts. Nevertheless, our results show that a Hofmeister series to certain degree, explain wet and dry fibrillar material systems following the direct interactions of ions with the surface of CNFs. Although more experimental efforts are needed to parameterize better the use specific ion effects in the rational assembly of high-performance nanostructures.

Acknowledgements

This study is funded by Knut and Alice Wallenberg Foundation through Wallenberg Wood Science Center. The authors are grateful to Prof. William D. Nix for fruitful discussions. N.M. acknowledge the kind support of Dr. Irene Linares Arregui from Department of Solid Mechanics at KTH with tensile test experiments.

Conflict of interest

The authors declare no conflict of interest.

Keywords: anions · Hofmeister series · mechanical properties · nanomaterials · self-assembly

How to cite: *Angew. Chem. Int. Ed.* **2019**, *58*, 18562 – 18569
Angew. Chem. **2019**, *131*, 18735 – 18742

[1] a) U. G. K. Wegst, H. Bai, E. Saiz, A. P. Tomsia, R. O. Ritchie, *Nat. Mater.* **2015**, *14*, 23; b) S. Ling, D. L. Kaplan, M. J. Buehler, *Nat. Rev. Mater.* **2018**, *3*, 18016; c) M. A. Meyers, P.-Y. Chen, A. Y. M. Lin, Y. Seki, *Prog. Mater. Sci.* **2008**, *53*, 1 – 206.

[2] W. Huang, D. Restrepo, J.-Y. Jung, F. Y. Su, Z. Liu, R. O. Ritchie, J. McKittrick, P. Zavattieri, D. Kisailus, *Adv. Mater.* **2019**, 1901561.

[3] a) Z. Gui, H. Zhu, E. Gillette, X. Han, G. W. Rubloff, L. Hu, S. B. Lee, *ACS Nano* **2013**, *7*, 6037 – 6046; b) Y. Li, F. Guo, Y. Hao, S. K. Gupta, J. Hu, Y. Wang, N. Wang, Y. Zhao, M. Guo, *Proc. Natl. Acad. Sci. USA* **2019**, *116*, 9245 – 9250; c) H. Ma, C. Burger, B. S. Hsiao, B. Chu, *J. Mater. Chem.* **2011**, *21*, 7507 – 7510.

[4] L. C. M. Lebreton, J. van der Zwet, J. W. Damsteeg, B. Slat, A. Andrady, J. Reisser, *Nat. Commun.* **2017**, *8*, 15611.

[5] N. Behabtu, C. C. Young, D. E. Tsentalovich, O. Kleinerman, X. Wang, A. W. K. Ma, E. A. Bengio, R. F. ter Waarbeek, J. J. de Jong, R. E. Hoogerwerf, S. B. Fairchild, J. B. Ferguson, B. Maruyama, J. Kono, Y. Talmon, Y. Cohen, M. J. Otto, M. Pasquali, *Science* **2013**, *339*, 182 – 186.

[6] a) C. W. Wang, D. Sinton, M. G. Moffitt, *J. Am. Chem. Soc.* **2011**, *133*, 18853 – 18864; b) N. Mittal, F. Ansari, K. Gowda V, C. Brouzet, P. Chen, P. T. Larsson, S. V. Roth, F. Lundell, L. Wågberg, N. A. Kotov, L. D. Söderberg, *ACS Nano* **2018**, *12*, 6378 – 6388.

[7] B. W. Ninham, *Adv. Colloid Interface Sci.* **1999**, *83*, 1 – 17.

[8] a) Y. Zhang, S. Furyk, D. E. Bergbreiter, P. S. Cremer, *J. Am. Chem. Soc.* **2005**, *127*, 14505 – 14510; b) P. Jungwirth, P. S. Cremer, *Nat. Chem.* **2014**, *6*, 261; c) F. Hofmeister, *Arch. Exp. Pathol. Pharmakol.* **1888**, *24*, 247 – 260.

[9] a) V. J. Nebot, J. J. Ojeda-Flores, J. Smets, S. Fernández-Prieto, B. Escuder, J. F. Miravet, *Chem. Eur. J.* **2014**, *20*, 14465 – 14472; b) R. S. Carnegie, C. L. D. Gibb, B. C. Gibb, *Angew. Chem. Int. Ed.* **2014**, *53*, 11498 – 11500; *Angew. Chem.* **2014**, *126*, 11682 – 11684; c) R. Du, Y. Hu, R. Hübner, J. O. Joswig, X. Fan, K. Schneider, A. Eychmüller, *Sci. Adv.* **2019**, *5*, eaaw4590; d) T. Benselfelt, M. Nordenström, M. M. Hamedi, L. Wågberg, *Nanoscale* **2019**, *11*, 3514 – 3520; e) A. J. Benítez, A. Walther, *Biomacromolecules* **2017**, *18*, 1642 – 1653; f) M. Shimizu, T. Saito, A. Isogai, *J. Membr. Sci.* **2016**, *500*, 1 – 7.

[10] N. Mittal, R. Jansson, M. Widhe, T. Benselfelt, K. M. O. Håkansson, F. Lundell, M. Hedhammar, L. D. Söderberg, *ACS Nano* **2017**, *11*, 5148 – 5159.

[11] M. Nordenström, A. Fall, G. Nyström, L. Wågberg, *Langmuir* **2017**, *33*, 9772 – 9780.

[12] A. Kamada, N. Mittal, L. D. Söderberg, T. Ingverud, W. Ohm, S. V. Roth, F. Lundell, C. Lendel, *Proc. Natl. Acad. Sci. USA* **2017**, *114*, 1232 – 1237.

[13] a) C. Brouzet, N. Mittal, F. Lundell, L. D. Söderberg, *Macromolecules* **2019**, *52*, 2286 – 2295; b) C. Brouzet, N. Mittal, L. D. Söderberg, F. Lundell, *ACS Macro Lett.* **2018**, *7*, 1022 – 1027.
[14] a) H. Dong, J. F. Snyder, K. S. Williams, J. W. Andzelm, *Biomacromolecules* **2013**, *14*, 3338 – 3345; b) K. S. Williams, J. W. Andzelm, H. Dong, J. F. Snyder, *Cellulose* **2014**, *21*, 1091 – 1101.
[15] a) U. Sivan, *Curr. Opin. Colloid Interface Sci.* **2016**, *22*, 1 – 7; b) D. F. Parsons, M. Bostrom, P. L. Nostro, B. W. Ninham, *Phys. Chem. Chem. Phys.* **2011**, *13*, 12352 – 12367; c) B. W. Ninham, P. L. Nostro, *Molecular Forces and Self Assembly: In Colloid, Nano Sciences and Biology*, Cambridge University Press, Cambridge, **2010**.
[16] V. Kocherbitov, *Carbohydr. Polym.* **2016**, *150*, 353 – 358.
[17] A. Sthoer, J. Hladílková, M. Lund, E. Tyrode, *Phys. Chem. Chem. Phys.* **2019**, *21*, 11329 – 11344.
[18] J. Grignon, A. M. Scallan, *J. Appl. Polym. Sci.* **1980**, *25*, 2829 – 2843.
[19] M. Boström, V. S. J. Craig, R. Albion, D. R. M. Williams, B. W. Ninham, *J. Phys. Chem. B* **2003**, *107*, 2875 – 2878.
[20] M. Henriksson, L. A. Berglund, P. Isaksson, T. Lindström, T. Nishino, *Biomacromolecules* **2008**, *9*, 1579 – 1585.
[21] A. J. Benítez, J. Torres-Rendon, M. Poutanen, A. Walther, *Biomacromolecules* **2013**, *14*, 4497 – 4506.
[22] H. Tang, N. Butchosa, Q. Zhou, *Adv. Mater.* **2015**, *27*, 2070 – 2076.
[23] T. Benselfelt, J. Engström, L. Wågberg, *Green Chem.* **2018**, *20*, 2558 – 2570.
[24] a) M. J. Lundahl, V. Klar, L. Wang, M. Ago, O. J. Rojas, *Ind. Eng. Chem. Res.* **2017**, *56*, 8 – 19; b) A. J. Benítez, A. Walther, *J. Mater. Chem. A* **2017**, *5*, 16003 – 16024; c) R.-B. Adusumali, M. Reifferscheid, H. Weber, T. Roeder, H. Sixta, W. Gindl, *Macromol. Symp.* **2006**, *244*, 119 – 125; d) S. Harish, D. P. Michael, A. Bensely, D. M. Lal, A. Rajadurai, *Mater. Charact.* **2009**, *60*, 44 – 49; e) M. F. Ashby, L. J. Gibson, U. Wegst, R. Olive, *Proc. R. Soc. London Ser. A* **1995**, *450*, 123 – 140.
[25] a) Y. Liu, A. Sponner, D. Porter, F. Vollrath, *Biomacromolecules* **2008**, *9*, 116 – 121; b) T. Vehoff, A. Glišović, H. Schollmeyer, A. Zippelius, T. Salditt, *Biophys. J.* **2007**, *93*, 4425 – 4432; c) Y. Liu, Z. Shao, F. Vollrath, *Nat. Mater.* **2005**, *4*, 901 – 905; d) C. H. Bowen, B. Dai, C. J. Sargent, W. Bai, P. Ladiwala, H. Feng, W. Huang, D. L. Kaplan, J. M. Galazka, F. Zhang, *Biomacromolecules* **2018**, *19*, 3853 – 3860.
[26] H. L. Gao, R. Zhao, C. Cui, Y. B. Zhu, S. M. Chen, Z. Pan, Y. F. Meng, S.-M. Wen, C. Liu, H. A. Wu, S. H. Yu, *Natl. Sci. Rev.* **2019**, doi.org/10.1093/nsr/nwz077.
[27] P. Mohammadi, M. S. Toivonen, O. Ikkala, W. Wagermaier, M. B. Linder, *Sci. Rep.* **2017**, *7*, 11860.
[28] N. Soykeabkaew, C. Sian, S. Gea, T. Nishino, T. Peijs, *Cellulose* **2009**, *16*, 435 – 444.
[29] A. Walther, J. V. I. Timonen, I. Díez, A. Laukkanen, O. Ikkala, *Adv. Mater.* **2011**, *23*, 2924 – 2928.
[30] T. Benselfelt, M. Nordenström, S. B. Lindström, L. Wågberg, *Adv. Mater. Interfaces* **2019**, *6*, 1900333.
[31] a) J. Barrett, *Inorganic chemistry in aqueous solution*, *Vol. 21*, Royal Society of Chemistry, London, **2003**; b) Y. Marcus, *J. Chem. Soc. Faraday Trans. 1* **1987**, *83*, 339 – 349; c) D. W. Smith, *J. Chem. Educ.* **1977**, *54*, 540.
[32] D. F. Parsons, B. W. Ninham, *J. Phys. Chem. A* **2009**, *113*, 1141 – 1150.
[33] M. Zhao, F. Ansari, M. Takeuchi, M. Shimizu, T. Saito, L. A. Berglund, A. Isogai, *Nanoscale Horiz.* **2018**, *3*, 28 – 34.
[34] G. I. Guerrero-García, P. González-Mozuelos, M. Olvera de la Cruz, *ACS Nano* **2013**, *7*, 9714 – 9723.
[35] Y. Ding, A. A. Hassanali, M. Parrinello, *Proc. Natl. Acad. Sci. USA* **2014**, *111*, 3310 – 3315.

Manuscript received: August 19, 2019
Revised manuscript received: October 1, 2019
Accepted manuscript online: October 10, 2019
Version of record online: November 4, 2019

